Atomic-Scale Distribution of Water Molecules at the Mica-Water Interface Visualized by Three-Dimensional Scanning Force Microscopy

Takeshi Fukuma,[1,2,3,*] Yasumasa Ueda,[3] Shunsuke Yoshioka,[3] and Hitoshi Asakawa[1]

[1]*Frontier Science Organization, Kanazawa University, Kakuma-machi, Kanazawa 920-1192, Japan*
[2]*PRESTO, Japan Science and Technology Agency, Honcho 4-1-9, Kawaguchi 332-0012, Japan*
[3]*Department of Electrical and Electronic Engineering, Kanazawa University, Kakuma-machi, Kanazawa 920-1192, Japan*

(Received 3 November 2009; published 6 January 2010)

We have developed a method referred to as three-dimensional scanning force microscopy (3D-SFM) which enables us to visualize water distribution at a solid-liquid interface with an atomic-scale resolution in less than 1 min. The 3D-SFM image obtained at a mica-water interface visualizes 3D distributions of adsorbed water molecules above the center of hexagonal cavities and the laterally distributed hydration layer. The atomically resolved 3D-SFM image showing mirror symmetry suggests the existence of surface relaxation of the cleaved mica surface next to the aqueous environment.

DOI: 10.1103/PhysRevLett.104.016101 PACS numbers: 68.37.Ps, 07.79.Lh

Muscovite mica (Fig. 1) is known as a prototype of clay minerals and hence has importance in fundamental research regarding clay swelling in geological science [1–3] and cloud seeding in ecological science [4,5]. In addition, owing to the ease of cleavage to present an atomically flat surface, a mica-water interface has been widely used as a model system to investigate nanofluidics in engineering and physics [6], lubrication in tribology, and molecular adsorption and diffusion in biology and chemistry. To date, the water distribution at a mica-water interface has been extensively studied by various techniques [7–13]. However, its atomistic model has not been established due to the difficulties in visualizing molecular-scale water distribution directly at a solid-liquid interface.

Scanning force microscopy (SFM) is a nanoscale imaging technique which visualizes an "isosurface" of an interaction force acting between a sharp tip and a surface as a two-dimensional (2D) image [Fig. 2(a)]. SFM has widely been used for imaging atomic-scale structures at solid-liquid, solid-air, and solid-vacuum interfaces. However, an interface inherently has a three-dimensional (3D) extent in subnanometer dimensions. Therefore, a 2D image obtained by SFM often fails to present important nature of interfacial phenomena. In particular, at a solid-liquid interface, solvent molecules interacting with a surface often show 3D local distribution, which has not been fully accessible with conventional 2D-SFM. Here we propose a method referred to as 3D-SFM [Fig. 2(b)], which enables us to visualize 3D distribution of water at a mica-water interface in 53 sec with an atomic-scale resolution. With the obtained 3D-SFM image, we discuss the 3D distribution of adsorbed water molecules and hydration layers as well as the atomic-scale structure of cleaved mica surface next to an aqueous environment.

Although the basic principles of 2D- and 3D-SFMs are applicable to various SFM operating modes, here we explain them in the case of frequency modulation (FM) detection mode [14], where the tip-sample interaction force is detected as a resonance frequency shift (Δf) of the vibrating cantilever. In 2D-SFM, the vertical tip position (z_t) is regulated to keep the Δf constant. With this tip-sample distance regulation, a tip is laterally scanned in XY to present a 2D height image of "Δf isosurface" having no vertical extent [Fig. 2(a)].

In 3D-SFM, a tip is scanned in Z as well as in XY to cover the whole 3D interfacial space [Fig. 2(b)]. z_t is modulated with a sine wave faster than the bandwidth of the distance regulation while the tip is laterally scanned. During the scan, Δf is recorded in real time with respect to the 3D tip positions while the averaged tip height (z_0) is regulated to keep the averaged Δf value constant. The 3D Δf image is constructed from either approaching or retracting Z profiles at each XY positions. The quantitative 3D force image is obtained by applying the force conversion formula [15] to the individual Z profiles constituting the 3D Δf image.

Previously reported 3D imaging techniques using SFM were developed based on 1D spectroscopy [16] or 2D constant height imaging [17–19] and hence have no tip-sample distance regulation during the measurement. In addition, owing to the complicated tip motion, these techniques take a measurement time on the order of hours or

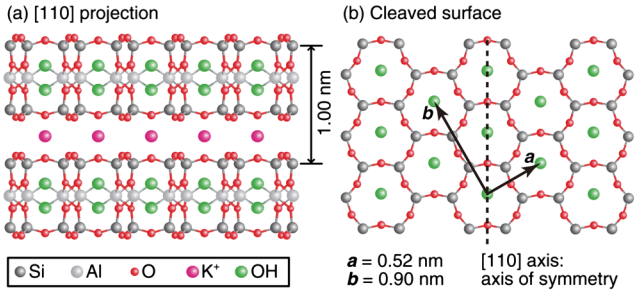

FIG. 1 (color online). Crystal structure of muscovite mica [$KAl_2(Si_3Al)O_{10}(OH)_2$] (Ref. [28]). (a) [110] projection. (b) Cleaved surface.

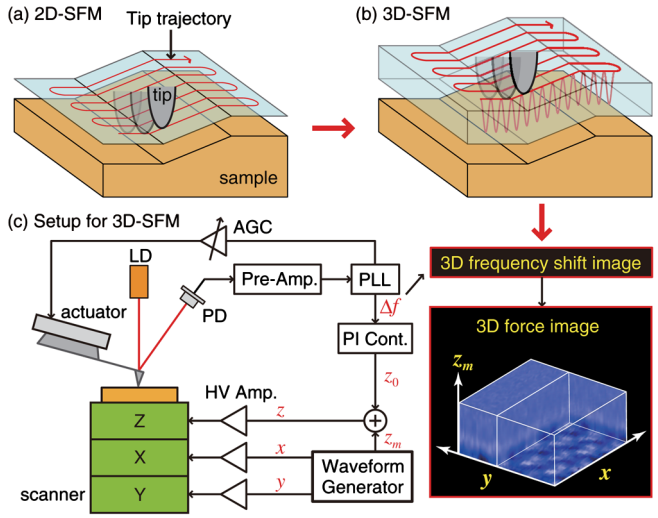

FIG. 2 (color online). Basic principles of (a) 2D-SFM and (b) 3D-SFM. (c) Experimental setup for the developed 3D-SFM. A phase-locked loop (PLL) circuit is used for the Δf detection while an automatic gain control (AGC) circuit is used for keeping the amplitude of the cantilever oscillation constant. The inset shows a 3D force image obtained at a mica-water interface ($2 \times 2 \times 0.78$ nm^3).

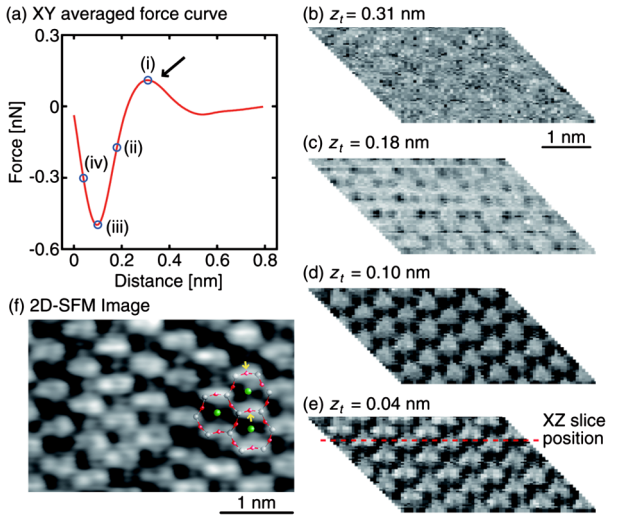

FIG. 3 (color online). 3D- and 2D-SFM images of mica-water interface obtained in PBS solution. (a) XY averaged force curve. The position for $z_t = 0$ is arbitrary. (b)–(e) XY cross sections of the 3D-SFM image at $z_t = 0.31$, 0.18, 0.10, and 0.04 nm, which, respectively, correspond to the z_t positions indicated by circles (i)–(iv) in (a). A linear drift correction was applied to the XY cross sections so that the periodic contrasts match the known lattice constants of a cleaved mica surface. The dotted line in (e) indicates the Y position of the XZ cross section shown in Fig. 4(a). (f) 2D-SFM image ($A = 0.26$ nm, $\Delta f = 67.1$ Hz) obtained with a different tip from the one used for the 3D-SFM imaging.

days. Therefore, it has been a great challenge to use these techniques in liquid at room temperature without tip crash or image distortions caused by the tip drift. On the contrary, 3D-SFM is developed based on 2D constant Δf imaging and hence has continuous tip-sample distance regulation feedback during the scan. In addition, the simple motion of the tip dramatically reduces the measurement time, which has allowed us to obtain an atomic-scale 3D image of mica-water interface in 53 sec.

The 3D-SFM imaging was performed at room temperature in phosphate buffered saline (PBS) solution. A Si cantilever (PPP-NCH: Nanoworld) with a resonance frequency of 123 kHz and a Q factor of 5.8 in liquid was used. The spring constant of the cantilever was estimated to be 14.2 N/m using the method in Ref. [20]. The 3D-SFM was developed by modifying the custom-built 2D-SFM with a low noise cantilever deflection sensor [21–23] [Fig. 2(c)]. The oscillation amplitude of the cantilever (A) was kept constant at 0.62 nm. The frequency and amplitude of the Z modulation during the 3D-SFM imaging were 200 Hz and 0.78 nm, respectively. The lateral scan speed was 12.2 nm/sec. Each XZ cross-sectional image was obtained in 0.32 sec while the whole 3D image was obtained in 53 sec. The 3D-SFM image ($4 \times 4 \times 0.78$ nm^3) was constructed from the approaching Z profiles and has $64 \times 64 \times 155$ pixels in XYZ.

Once complete 3D force field is obtained, we are able to extract any 1D profiles or 2D cross sections. An XY averaged force curve was obtained by plotting force values averaged over an XY cross section at each z_t [Fig. 3(a)]. This curve shows an oscillatory profile with a peak [arrow in Fig. 3(a)] having a width of 0.2–0.3 nm, which agrees with the diameter of a water molecule. Owing to this agreement and previous studies on mica-water interface [24,25], we attributed the repulsive peak to the interaction with a hydration layer. This interpretation is further supported by the discussion described later.

From XY cross sections at different z_t [Figs. 3(b)–3(e)], continuous z_t dependence of XY force distribution is obtained [26]. The XY cross section in Fig. 3(b) does not show any contrast, which reveals the uniform lateral distribution of water molecules in the hydration layer. As the tip approaches the surface, the XY cross section shows an atomic-scale contrast [Figs. 3(c)–3(e)], reflecting the appearance of the short-range interaction force between the tip front atom and the atoms constituting the mica surface. With further decrease of z_t, the hexagonally arranged force peaks found in Fig. 3(d) turn into pairs of smaller peaks [Fig. 3(e)].

The periodic pairs of the force peaks found in Fig. 3(e) appear to be uniform, which gives rise to a question whether the contrast represents the structure of mica surface or the tip apex [27]. However, we confirmed that a similar contrast is reproduced in a 2D-SFM image obtained with a different tip as shown in Fig. 3(f). In the image, the height of individual atoms has irregular variations, which strongly suggests that the contrast is unlikely to be origi-

nated from a tip artifact. By comparing the image shown in Fig. 3(f) and the atomic-scale model of mica [Fig. 1(b)], we attributed the observed pairs of force peaks to the repulsive forces measured on the two adjacent Si atoms as indicated by the model overlaid on the image in Fig. 3(f). The height variations of the individual peaks are likely to represent the difference between Si and Al atoms as reported previously [25].

The 3D- and 2D-SFM images consistently show an atomic-scale contrast with mirror symmetry. This is an important finding since a cleaved mica surface is often considered to have sixfold symmetry. Strictly speaking, this is inaccurate. The atomic-scale model derived from x-ray diffraction data [28] shows that a cleaved mica surface does not have sixfold symmetry but has mirror symmetry. However, the feature found in the SFM images is more evident than expected from the atomic-scale model. This is because two of the six oxygen atoms constituting the hexagonal ring, which are indicated by arrows in Fig. 3(f), are imaged with a brighter contrast than that of the other four atoms. Such difference from the atomic-scale model obtained with a bulk crystal indicates the existence of surface relaxation at mica-water interface.

Another remarkable feature found in the SFM images is an enhanced contrast at the center of the cavity surrounded by a hexagonal ring. The overlaid model shown in Fig. 3(f) reveals that the XY position of the enhanced contrast corresponds to that of an OH group located at the bottom of the cavity. The vertical corrugation of the mica surface makes it difficult to analyze correlation between the atomic-scale structure and the force distribution with a 2D-SFM image having no vertical extent. Such an analysis becomes possible by extracting a vertical cross section from a 3D-SFM image as shown in Fig. 4(a) [26]. The left half of the XZ cross section is shown with a low contrast to visualize the localized force distribution above a OH group while the right half of the image is shown with a high contrast to visualize the layerlike force distribution over the entire surface. The layerlike force distribution corresponds to the repulsive peak indicated by the arrow in Fig. 3(a) and has been attributed to the hydration layer.

By extracting individual Z profiles constituting the XZ cross section, site specific force profiles are obtained as shown in Fig. 4(b). The Z profiles show strong site dependence especially at the Z distance range $z_t < 0.2$ nm. Profile 1 shows a large attractive force due to the absence of an underlying atom. Profile 2 shows a relatively broad repulsive peak due to the localized force distribution above an OH group. On the contrary, Profile 3 shows a shallow and broad attractive peak due to the competition between the attractive van der Waals or hydration force and a repulsive interaction force between the tip and the Si atom. This means that the repulsive force component measured on the Si site starts to increase at a higher z_t than it does on the OH site owing to their height difference.

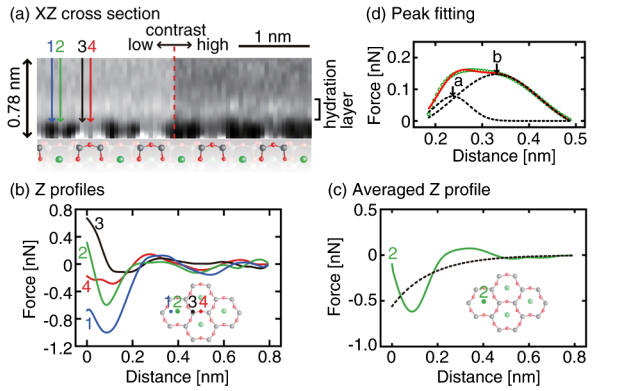

FIG. 4 (color online). XZ cross section and Z profiles of 3D-SFM image of mica-water interface obtained in PBS solution. (a) XZ cross section obtained at the Y position indicated by a dotted line in Fig. 3(e). An atomic-scale model of [110] projection of muscovite mica is shown below the XZ cross section. (b) Z profiles measured along Line 1–4 indicated in (a). (c) An average of 48 Z profiles measured on OH sites. The dotted line was obtained by fitting the curve with an exponential function. The insets in (b) and (c) show the measurement positions for the Z profiles. (d) The circles show the peak profile obtained by subtracting the dotted line in (c) from the solid line in (c). The dotted lines show the double Gaussian peak profiles obtained by fitting the peak profile. z_t values for Peaks a and b are 0.237 and 0.331 nm, respectively. The solid line shows summation of the two dotted lines.

In spite of the similar Z positions of Si and O, Profiles 3 and 4 show remarkably different features. Profile 4 does not present a repulsive force branch but an almost constant force for the Z distance range $z_t = 0$–0.15 nm. At a cleaved mica surface, the Si atom is strongly supported by tetrahedrally arranged four chemical bonds, while the O atom is supported only by two chemical bonds, leaving a larger flexibility. Therefore, the repulsive force between an O atom and an approaching tip may be strong enough to displace the O atom, which accounts for the constant force regime observed in Profile 4.

Profile 2 shows a relatively broad repulsive peak due to the influence of the localized force distribution above an OH group. To quantitatively analyze the peak profile, 48 Z profiles measured on OH sites are extracted from the 3D-SFM image and averaged to obtain a smoothed profile [Fig. 4(c)]. The averaged curve was fitted with an exponential function to obtain a long-range background component as indicated by the dotted line in Fig. 4(c). This long-range component is subtracted from the averaged force profile to obtain the peak profile as shown in Fig. 4(d). The peak presents a broad profile with a plateau on top of it, which does not appear to be a single peak but a summation of double peaks. Thus, we fitted the peak profile with double Gaussian peaks as indicated by the dotted lines in Fig. 4(d). According to the fitting parameters, the minor peak at $z_t = 0.237$ nm (Peak a) has a width of 0.103 nm

while the major peak at $z_t = 0.331$ nm (Peak b) has a width of 0.258 nm.

Note that the long-range force at a solid-liquid interface include various components such as van der Waals force, monotonic solvation forces, and electric double layer force [29]. Since these components have different distance dependences, the choice of fitting function is not trivial. However, we confirmed that the use of different fitting functions such as $1/z_t$ results in a minor change in the distance values obtained above and hence does not influence the following discussions.

So far, some of the previous studies on the mica-water interface supported the existence of ''icelike'' water [7–9] while others suggested the existence of more disordered ''liquidlike'' water [10,11]. Recently, studies using x-ray reflectometry [12] and Monte Carlo simulation [13] consistently suggested the existence of adsorbed water molecules presenting localized water distribution above OH groups in addition to the laterally distributed hydration layer. The water density profiles obtained in these previous studies revealed that the Z distance between the peaks corresponding to the hydration layer and adsorbed water molecules is 0.12 nm. This value approximately agrees with the peak distance (0.094 nm) measured in Fig. 4(d), which indicates that the enhanced contrast measured on OH sites should represent the localized distribution of adsorbed water molecules.

Therefore, the results obtained in this study support the model proposed by Cheng *et al.* [12], where the adsorbed and laterally distributed water molecules coexist at the interface. The coexistence of water molecules having a long relaxation time (adsorbed water) and laterally distributed disordered water molecules (2D hydration layer) may reconcile the two opposing ideas of ''icelike'' and ''liquidlike'' water molecules at the mica-water interface.

The basic principle of 3D-SFM is applicable to other scanning probe techniques in other environments. Even with the results obtained on an atomically flat interface, the necessity of the 3D imaging is evident as seen in this study. This requirement should become more evident when it is applied to biological systems having a larger corrugation and inhomogeneity. One of the attractive applications in this respect is to visualize 3D distribution of hydration structure around a protein, which should provide new insights into the roles of water in biological functions.

This research was supported by PRESTO, Japan Science and Technology Agency.

*fukuma@staff.kanazawa-u.ac.jp

[1] *Review in Mineralogy: Mineral Water Interface Geochemistry*, edited by M. Hochella, Jr. and A. F. White (Mineralogical Society of America, Chantilly, VA, 1990).
[2] E. S. Boek, P. V. Coveney, and N. T. Skipper, J. Am. Chem. Soc. **117**, 12 608 (1995).
[3] S. Karaborni, B. Smit, W. Heidug, J. Urai, and E. van Oort, Science **271**, 1102 (1996).
[4] G. R. Edwards, L. F. Evans, and A. F. Zipper, Trans. Faraday Soc. **66**, 220 (1970).
[5] J. L. Caslavsky and K. Vedam, J. Appl. Phys. **42**, 516 (1971).
[6] Y. Leng and P. T. Cummings, J. Chem. Phys. **124**, 074711 (2006).
[7] G. Sposito and R. Prost, Chem. Rev. **82**, 553 (1982).
[8] M. Odelius, M. Bernasconi, and M. Parrinello, Phys. Rev. Lett. **78**, 2855 (1997).
[9] P. B. Miranda, L. Xu, Y. R. Shen, and M. Salmeron, Phys. Rev. Lett. **81**, 5876 (1998).
[10] R. Bergman and J. Swenson, Nature (London) **403**, 283 (2000).
[11] J. Swenson, R. Bergman, and W. Howells, J. Chem. Phys. **113**, 2873 (2000).
[12] L. Cheng, P. Fenter, K. L. Nagy, M. L. Schlegel, and N. C. Sturchio, Phys. Rev. Lett. **87**, 156103 (2001).
[13] S.-H. Park and G. Sposito, Phys. Rev. Lett. **89**, 085501 (2002).
[14] T. R. Albrecht, P. Grütter, D. Horne, and D. Ruger, J. Appl. Phys. **69**, 668 (1991).
[15] J. E. Sader and S. P. Jarvis, Appl. Phys. Lett. **84**, 1801 (2004).
[16] H. Hölscher, S. M. Langkat, A. Schwarz, and R. Wiesendanger, Appl. Phys. Lett. **81**, 4428 (2002).
[17] B. J. Albers, T. C. Schwendemann, M. Z. Baykara, N. Pilet, M. Liebmann, E. I. Altman, and U. D. Schwarz, Nature Nanotech. **4**, 307 (2009).
[18] M. Ternes, C. P. Lutz, C. F. Hirjibehedin, F. J. Giessibl, and A. J. Heinrich, Science **319**, 1066 (2008).
[19] L. Gross, F. Mohn, P. Liljeroth, J. Repp, F. J. Giessibl, and G. Meyer, Science **324**, 1428 (2009).
[20] J. L. Hutter and J. Bechoefer, Rev. Sci. Instrum. **64**, 1868 (1993).
[21] T. Fukuma, M. Kimura, K. Kobayashi, K. Matsushige, and H. Yamada, Rev. Sci. Instrum. **76**, 053704 (2005).
[22] T. Fukuma and S. P. Jarvis, Rev. Sci. Instrum. **77**, 043701 (2006).
[23] T. Fukuma, Rev. Sci. Instrum. **80**, 023707 (2009).
[24] J. N. Israelachvili and G. E. Adams, Nature (London) **262**, 774 (1976).
[25] T. Fukuma, K. Kobayashi, K. Matsushige, and H. Yamada, Appl. Phys. Lett. **87**, 034101 (2005).
[26] See supplementary material at http://link.aps.org/supplemental/10.1103/PhysRevLett.104.016101 for movies showing the XY and XZ cross sections of the 3D-SFM image obtained at mica/water interface.
[27] F. J. Giessibl, S. Hembacher, H. Bielefeldt, and J. Mannhart, Science **289**, 422 (2000).
[28] S. M. Richardson and J. W. Richardson, Am. Mineral. **67**, 69 (1982).
[29] J. N. Israelachvili, *Intermolecular and Surface Forces* (Academic Press Ltd., London, 1992).